Resonant radiation in synchronously pumped passive Kerr cavities

Kathy Luo,[1] Yiqing Xu,[2] Miro Erkintalo,[1] and Stuart G. Murdoch[1,*]

[1] *Physics Department, The University of Auckland, Private Bag 92019, Auckland 1142, New Zealand*
[2] *Department of Electrical and Electronic Engineering, The University of Hong Kong, Pokfulam Road, Hong Kong, China.*
[*] *Corresponding author: s.murdoch@auckland.ac.nz*

Compiled September 30, 2014

We report theoretical, numerical and experimental studies of resonant dispersive wave (DW) generation in synchronously pumped passive Kerr resonators. Our results demonstrate that multiple DWs can be simultaneously excited when pumping in either the anomalous or normal dispersion regimes. They correspond to the fundamental DW that propagates phase-matched to the pump, and to higher-order Kelly-like sidebands whose resonant amplification is permitted by the cavity periodicity. In addition, we experimentally confirm that the DW frequencies can be controlled by adjusting the phase detuning between the pump and the cavity. Our experimental measurements are in excellent agreement with numerical simulations and derived phase-matching conditions.

OCIS codes: (140.3510) Lasers, fiber; (140.7090) Ultra-fast lasers; (060.5530) Pulse propagation and solitons.

The generation of resonant dispersive waves (DWs) is a central process in nonlinear optics [1, 2], with important implications to fiber supercontinuum generation [3–5], novel wave propagation phenomena [6–8], mode-locked lasers [9–12], and microresonator frequency combs [13–15]. It describes the transfer of energy from a strong pump to a weak linear wave, and occurs when the dispersion of the nonlinear medium permits phase-matching between the interacting fields. The majority of studies have considered soliton-like pumps propagating in the anomalous dispersion regime, but recently it has been shown that even a normal-dispersion pump is capable of emitting a weak anomalous-dispersion DW [16–18].

In conventional waveguide configurations only radiation that propagates in-phase with the pump is amplified, which typically gives rise to a single emitted DW [1, 3]. To the contrary, in periodic systems also radiation that is quasi phase-matched can couple to the pump, which can lead to multiple DWs. Kelly sidebands in mode-locked fiber lasers represent an archetypical example [9–11], yet similar sidebands can occur under any form of periodic perturbation [19]. In particular, both fundamental and quasi-phasematched DWs have been predicted in the anomalous dispersion regime of a coherently-driven passive resonator [13, 20], which has attracted interest in the context of frequency comb generation in high-Q microresonators [13–15]. More recently cavity DWs have also been predicted in the normal dispersion regime, where they are emitted by mixed dispersive-dissipative shock waves [21]. A unique feature of these systems is that the detuning between the input pump and the modes of the cavity assumes an important role in the phase-matching condition governing the DW emission process [15]. Despite the growing interest, however, DW generation in passive resonators has only recently been studied experimentally [22]. These experiments relied on temporal cavity solitons [23–25], and as consequence were restricted to anomalous dispersion pumping and to a constant cavity detuning. Phase-dependent dynamics have been observed in feedback-assisted supercontinuum generation [26, 27], but the effect on DW characteristics was not discussed, and no comparison with phase-matching predictions presented.

In this Letter, we report a full experimental study of DW generation in a coherently-driven passive resonator. In contrast to [22], here we synchronously pump the resonator using a wavelength-tunable mode-locked laser, which allows us to explore both normal and anomalous dispersion pumping. In both regimes we observe simultaneous excitation of fundamental and higher-order quasi phase-matched DWs. Our configuration enables flexible control over the cavity detuning, permitting us to verify its key role in governing the DW resonance frequencies and to identify a range of new phase-matching features.

We consider a passive resonator with Kerr nonlinearity, pumped with a pulse source centered at ω_0 whose repetition rate is synchronized to the free-spectral range of the cavity. Constructive interference at the input coupler can lead to coherent transfer of power from the pump to a linear DW, provided that the phase difference they accumulate over a single roundtrip is equal to $2\pi m$ (m is an integer). During the time t_R it takes for the intracavity field to complete a single roundtrip, the phase of the pump at the coupler changes by $\phi_\mathrm{p} = -\omega_0 t_\mathrm{R}$, whilst an intracavity component at ω acquires an additional component due to propagation over the ring $\phi_\mathrm{s} = \beta(\omega)L - \omega t_\mathrm{R}$, where $\beta(\omega)$ is the propagation constant in the medium and L the length of the loop. Requiring $\phi_\mathrm{s} = \phi_\mathrm{p} + 2\pi m$, we obtain a phase-matching condition that governs the frequency of resonant DWs:

$$\sum_{k\geq 2} \frac{\beta_k}{k!}(\omega-\omega_0)^k L = 2\pi m + \delta_0. \tag{1}$$

Here the β_k's are the dispersion coefficients associated with the Taylor series expansion of $\beta(\omega)$ about ω_0 [3], and $\delta_0 = 2\pi k - \phi_0$ with $\phi_0 = \beta_0 L$ describes the phase

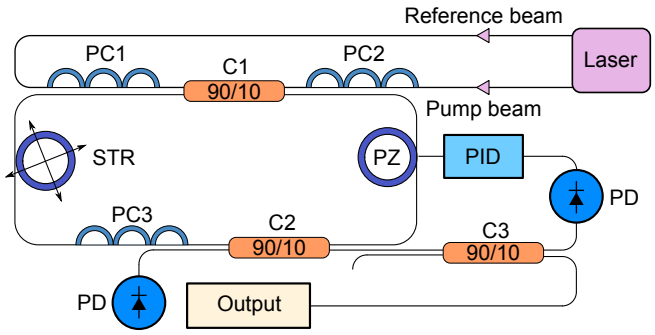

Fig. 1. (Color online) Schematic diagram of the experimental setup. PC, fiber polarization controller; C, 90/10 fiber coupler; STR, static fiber stretcher; PZ, dynamic piezo-electric fiber stretcher; PID; feedback electronics; PD, photodiode.

detuning of the pump wavelength from the closest cavity resonance with order k [28]. In lasers $\delta_0 = 0$, and Eq. (1) reduces to the expression describing the frequency detuning of Kelly sidebands [9–11]. If the pump repetition time t_P is not fully synchronised with the cavity, such that $\Delta t = t_\mathrm{R} - t_\mathrm{P} \neq 0$, an extra term $(\omega - \omega_0)\Delta t$ appears on the right-hand side of Eq. (1). This term is equivalent to the usual group-velocity mismatch term that arises when the DW generating pump is not centered at ω_0 (about which $\beta(\omega)$ is expanded) [3, 18], but here it manifests itself due to pump-cavity desynchronization.

To experimentally study the process, we use the setup shown in Fig. 1. It is conceptually similar to the one used to study cavity modulation instability in [28,29], and corresponds to a synchronously-pumped, phase-stabilized resonator constructed of 10.3 m loop of single-mode optical fiber, closed on itself with 90/10 input couplers. We control the overall dispersion of the cavity by using two different types of fiber: (i) standard SMF-28 with second- and third-order dispersion coefficients $\beta_2 = -19.8$ ps^2/km and $\beta_3 = 0.1$ ps^2/km, respectively, and (ii) a dispersion-shifted fiber (Corning MetroCor) with $\beta_2 = 7.0$ ps^2/km and $\beta_3 = 0.1$ ps^2/km at 1550 nm. Note that dispersion coefficients beyond the third order are negligible for these fibers and can be neglected ($\beta_k = 0$ for $k \geq 4$). Moreover, whilst our cavity is constructed from two different fibers Eq. (1) still remains valid, provided that the dispersion coefficients used correspond to mean values of the cavity. The resonator is pumped with a wavelength-tunable 20 MHz passively mode-locked fiber laser (Calmar FPL-02C). The pulse width and peak power at the input to the cavity is estimated to be 600 fs (FWHM) and 250 W, respectively. The pump is coupled into the ring via the 90/10 coupler C1 and circulates in an anti-clockwise direction.

To synchronize the repetition rate of the pump laser to the fiber loop we adjust the cavity length using a static fiber stretcher. Moreover, a dynamic piezo-electric stretcher and a commercial PID circuit (SRS SIM960) are used to stabilize the average out-coupled power at a set level, ensuring that the detuning between the laser and the cavity is locked to a fixed value. Owing to the large (of the order of π) Kerr-induced phase tilt of the cavity resonance [28], we can access a wide range of detunings δ_0. This should be contrasted with experiments performed with temporal cavity solitons, whose sensitivity to cavity detuning prevents large δ_0 excursions [22].

The locking system ensures constant detuning but does not reveal its value. To measure it we use a technique similar to that in [28, 29]. Specifically, a weak (5%) copy of the pump acts as a linear reference beam that is simultaneously coupled into the loop, propagating in the opposite direction than the main pump (here clockwise). Because this weak beam does not experience any Kerr tilt, the cavity lengths at which its resonances peak correspond to $\delta_0 = 0$, for both the clockwise and anti-clockwise beams. (This is confirmed by dropping the power of the main pump to 5% and verifying that their resonances coincide.) By scanning the piezo-electric stretcher we can then compare the distance between a linear peak and the lock point (l) to the separation between consecutive linear peaks (l'). This allows us to calculate the value of the cavity detuning as $\delta_0 = 2\pi l/l'$.

In addition to experiments we perform numerical simulations using a full iterative cavity map, where propagation through each fiber segment is modelled using a generalized nonlinear Schrödinger equation [3]. The pump is coherently added to the intracavity field in the beginning of each roundtrip (with appropriate detuning), and we include output coupling as well as splice losses so as to match the finesse of the modelled cavity with that measured experimentally.

We first consider pumping in the anomalous dispersion regime. To this end, we construct a loop consisting of 7.12 m of MetroCor fiber and 3.18 m of SMF-28, which sets the net cavity zero dispersion wavelength (ZDW) to 1534 nm. We measured the finesse of this cavity to be $\mathcal{F} \sim 18$. The pump wavelength was tuned to 1542 nm where the net dispersion is anomalous with $\bar{\beta}_2 = -0.64$ ps^2/km. In Fig. 2(a) we plot the spectrum exiting the loop with the cavity detuning locked to $\delta_0 = 1.46$ rad. We can see that the spectrum shows multiple fine features and sharp DW-like peaks that are absent at the input. Figure 2(b) shows the output spectrum obtained from numerical simulations, and it is in good qualitative agreement with the experiment. The roundtrip-to-roundtrip evolution of the simulated spectrum is shown in Fig. 2(c), and the system is seen to reach a steady state in approximately 30 roundtrips. In Fig. 2(b) we also highlight, as dashed lines, the theoretically predicted DW frequencies given by the linear phase-matching Eq. (1). These predictions are in excellent agreement with the observed positions, validating their origins as resonant DWs. They are also in good agreement with experimentally observed DW shifts for the fundamental ($m = 0$, $\lambda_0 = 1506$ nm) and positive-order ($m = 1$, $\lambda_1 = 1490$ nm; $m = 2$, $\lambda_2 = 1481$ nm) DWs. For the negative-order DWs, we tentatively identify the experimentally observed peaks at 1582 nm and 1594 nm as the $m = -2$ and $m = -3$ quasi-phasematched DWs

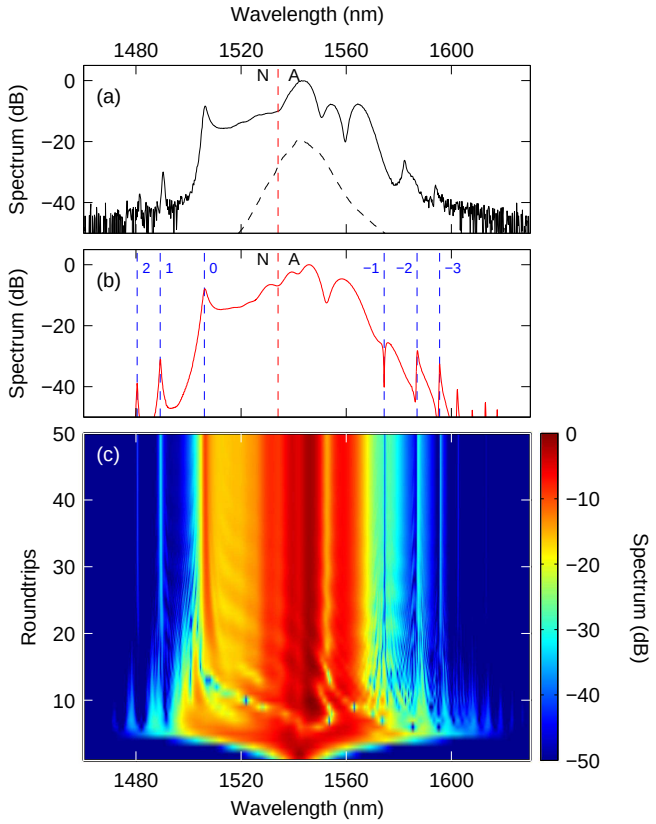

Fig. 2. (Color online) (a,b) Resonator output spectrum measured experimentally (a) and extracted from numerical simulations (b). The net ZDW (1534 nm) is marked by the red dashed line. The dashed black curve in (a) is the input spectrum (vertically offset for clarity). Predictions from linear phase-matching equation are shown as dashed blue lines in (b). (c) Evolution of the simulated spectrum at the output of the fiber loop as a function of roundtrip number.

respectively, with the $m = -1$ dispersive wave absent. We believe the discrepancy between predicted and observed shifts for these DWs is due to our somewhat limited knowledge of the fiber characteristics.

We next investigate the generation of DWs when pumping in the normal dispersion regime. To this end, we construct a second cavity consisting of 7.95 m of MetroCor fiber and 2.35 m of SMF-28, which sets the ZDW at 1561 nm. The finesse of this cavity was measured to be $\mathcal{F} \sim 12$. To access normal dispersion, we set the pump wavelength to 1556 nm where the average GVD coefficient $\bar{\beta}_2 = +0.42$ ps^2/km. In Fig. 3(a) we plot the measured output spectrum when the cavity detuning was locked at $\delta_0 = 1.28$ rad. Interestingly, we can identify a fundamental DW at 1534 nm, which is well within the *normal* dispersion regime. At first this may seem surprising, since a normal-dispersion pump is forbidden to emit a DW into the normal dispersion regime under previously studied configurations [16–18]. Here, however, this process is permitted due to the presence of the (positive) cavity detuning parameter in Eq. (1). We indeed observe an identical feature in the numerically simulated spectrum, shown in Fig. 3(b), where we also confirm it to

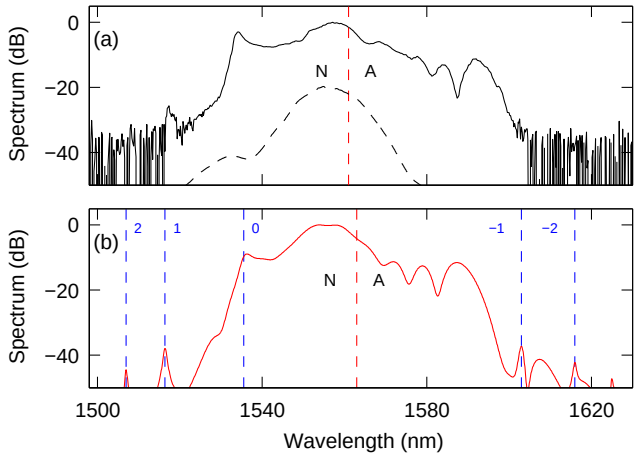

Fig. 3. (Color online) (a,b) Resonator output spectrum measured experimentally (a) and extracted from numerical simulations (b) when pumping in the normal dispersion regime. The dashed curves have meaning identical to those in Fig. 2.

correspond to a fundamental DW by highlighting how its position is accurately predicted by Eq. (1) with $m = 0$. In addition to the fundamental DW, our experiments also display a single higher-order quasi phase-matched DW ($m = 1$) at 1517 nm, which is in good agreement with numerical simulations and theoretical predictions. The simulated spectrum additionally shows the presence of several weak negative-order DWs. These are not observed experimentally, presumably as they fall below the noise floor of our optical spectrum analyzer.

To complete our study we investigate in more detail how the cavity detuning δ_0 affects the DW frequencies. For simplicity we consider only the fundamental and the clearly experimentally identifiable positive-order DWs. We perform experiments in both the normal and the anomalous dispersion regimes (using the same parameters as in the experiments above), and we systematically vary the cavity detuning over the full range of experimentally accessible values. This range is set for low δ_0 by the lack of power coupled into the cavity, leading to negligible nonlinear effects and no DWs, and for large δ_0 by our inability to lock the fiber loop too close to the peak of the tilted resonance. For each accessible value we extract the frequency detunings Δf between the pump and the generated DWs.

Results corresponding to pumping in the normal and in the anomalous dispersion regime are summarized in Figs. 4(a) and (b), respectively. Here, we compare the DW frequencies extracted from experimentally recorded spectra (open circles), with predictions of Eq. (1) (solid curves). With anomalous-dispersion pumping, we see how the fundamental DW is predicted to exhibit a comparatively small variation for experimentally accessible detunings, shifting from 4.6 THz at $\delta_0 = 1.4$ rad to 5.2 THz at $\delta_0 = 2.4$ rad. This is in reasonably good agreement with experimental observations. We also show predicted and measured DW frequencies for the first three positive-order sidebands, and observe similar trends and

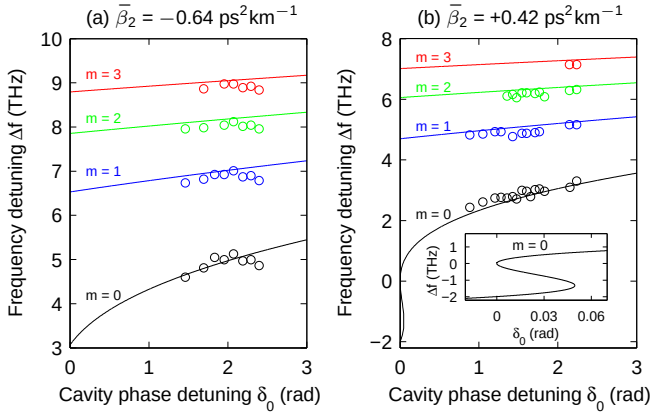

Fig. 4. (Color online) Measured (open circles) and predicted (solid lines) DW frequency shifts as a function of cavity phase detuning for (a) $\bar{\beta}_2 = -0.64$ ps^2/km, and (b) $\bar{\beta}_2 = +0.42$ ps^2/km. Inset in (b) is a zoom on the $\delta_0 \sim 0$ region.

agreement. Note that although the variation for experimental detunings is small, the overall difference from the single-pass prediction (with $\delta_0 = 0$) is more than 2 THz, highlighting the key role of the cavity phase detuning.

When pumping in the normal dispersion regime we observe a stronger detuning-dependence [see Fig. 4(b)], with the frequency of the fundamental DW changing from 2.2 to 3.3 THz over the experimentally accessible values. This is in good agreement with the theoretical predictions. We can also see that, for cavity detunings close to zero, the phase-matching Eq. (1) actually permits three distinct fundamental $m = 0$ DWs (see inset). At $\delta_0 = 0$ the frequency shifts of the blue-shifted solution and one of the red-shifted solutions fall to zero. This simply highlights that without the cavity detuning parameter, a normal-dispersion pump can only generate a single, anomalous-dispersion DW [16–18]. Unfortunately, this region is not accessible with our current setup because of low power transfer into the cavity for small δ_0. We note however that increasing $\bar{\beta}_2$ or decreasing $\bar{\beta}_3$ would extend the region where these solutions exist, and so it may be possible in the future to study this regime using a differently designed cavity. Finally, multiple $m = 0$ DWs are predicted to occur also in the anomalous dispersion regime, provided that $\delta_0 < 0$.

In conclusion, we have investigated the generation of dispersive waves in a passive Kerr cavity. We have shown both theoretically and experimentally that the cavity phase detuning provides an extra degree of freedom that can give rise to previously unreported phase-matching features. Using a synchronously pumped fiber cavity, we have experimentally observed fundamental and quasi phase-matched DWs when pumping both in the anomalous and in the normal dispersion regime. Their measured properties have been found to be in good agreement with numerical simulations and theoretical predictions based on phase-matching considerations. Our results could to lead to a better understanding of DW generation in periodic systems and passive resonators.

We acknowledge support from the Marsden Fund of the Royal Society of New Zealand.

References

1. P. K. A. Wai, C. R. Menyuk, Y. C. Lee, and H. H. Chen, Opt. Lett. **11**, 464–466 (1986).
2. N. Akhmediev and M. Karlsson, Phys. Rev. A **51**, 2602–2607 (1995).
3. J. M. Dudley, G. Genty, and S. Coen, Rev. Mod. Phys. **78**, 1135–1184 (2006).
4. D. V. Skryabin and A. V. Gorbach, Rev. Mod. Phys. **82,** 1287–1299 (2010).
5. J. C. Travers, J. Opt. **12**, 113001 (2010).
6. M. Erkintalo, G. Genty, and J. M. Dudley, Opt. Express **18**, 13379–13384 (2010).
7. A. Mussot, A Kudlinski, M. Droques, P. Szriftgiser, and N. Akhmediev, Phys. Rev. X **4**, 011054 (2014).
8. T. Roger, D. Majus, G. Tamosauskas, P. Panagiotopoulos, M. Kolesik, G. Genty, A. Dubietis, and D. Faccio, arXiv:1404.0937 [physics] (2014).
9. S. Kelly, Electronics Letters **28**, 806–807 (1992).
10. N. Smith, K. Blow, and I. Andonovic, Journal of Lightwave Technology **10**, 1329–1333 (1992).
11. M. Dennis and I. Duling, I.N., IEEE Journal of Quantum Electronics **30**, 1469–1477 (1994).
12. P. F. Curley, C. Spielmann, T. Brabec, F. Krausz, E. Wintner, and A. J. Schmidt, Opt. Lett. **18**, 54–56 (1993).
13. S. Coen, H. G. Randle, T. Sylvestre, and M. Erkintalo, Opt. Lett. **38**, 37–39 (2013).
14. M. R. E. Lamont, Y. Okawachi, and A. L. Gaeta, Opt. Lett. **38**, 3478–3481 (2013).
15. C. Milián and D. Skryabin, Optics Express **22**, 3732 (2014).
16. M. Erkintalo, Y. Q. Xu, S. G. Murdoch, J. M. Dudley, and G. Genty, Phys. Rev. Lett. **109**, 223904 (2012).
17. K. E. Webb, Y. Q. Xu, M. Erkintalo, and S. G. Murdoch, Opt. Lett. **38**, 151–153 (2013).
18. M. Conforti and S. Trillo, Opt. Lett. **38**, 3815–3818 (2013).
19. J. P. Gordon, Journal of the Optical Society of America B **9**, 91 (1992).
20. R. Valle, Optics Communications **93**, 389–399 (1992).
21. S. Malaguti, M. Conforti, and S. Trillo, Opt. Lett. **39**, 5626-5629 (2014).
22. J. K. Jang, M. Erkintalo, S. G. Murdoch, and S. Coen, Opt. Lett. **39**, 5503-5506 (2014).
23. S. Wabnitz, Opt. Lett. **18**, 601–603 (1993).
24. F. Leo, S. Coen, P. Kockaert, S.-P. Gorza, P. Emplit, and M. Haelterman, Nat Photon **4**, 471–476 (2010).
25. J. K. Jang, M. Erkintalo, S. G. Murdoch, and S. Coen, Nat Photon **7**, 657–663 (2013).
26. N. Brauckmann, M. Kues, P. Groß, and C. Fallnich, Opt. Express **18**, 24611–24618 (2010).
27. P. Groß, N. Haarlammert, M. Kues, T. Walbaum, and C. Fallnich, Opt. Fiber. Technol. **18**, 290–303 (2012).
28. S. Coen, M. Haelterman, P. Emplit, L. Delage, L. M. Simohamed, and F. Reynaud, J. Opt. Soc. Am. B **15**, 2283–2293 (1998).
29. S. Coen and M. Haelterman, Phys. Rev. Lett. **79**, 4139–4142 (1997).

Informational Fifth Page

References

1. P. K. A. Wai, C. R. Menyuk, Y. C. Lee, and H. H. Chen, "Nonlinear pulse propagation in the neighborhood of the zero-dispersion wavelength of monomode optical fibers," Opt. Lett. **11**, 464–466 (1986).
2. N. Akhmediev and M. Karlsson, "Cherenkov radiation emitted by solitons in optical fibers," Phys. Rev. A **51**, 2602–2607 (1995).
3. J. M. Dudley, G. Genty, and S. Coen, "Supercontinuum generation in photonic crystal fiber," Rev. Mod. Phys. **78**, 1135–1184 (2006).
4. D. V. Skryabin and A. V. Gorbach, "Colloquium: Looking at a soliton through the prism of optical supercontinuum," Rev. Mod. Phys. **82,** 1287–1299 (2010).
5. J. C. Travers, "Blue extension of optical fibre supercontinuum generation," J. Opt. **12**, 113001 (2010).
6. M. Erkintalo, G. Genty, and J. M. Dudley, "Experimental signatures of dispersive waves emitted during soliton collisions," Opt. Express **18**, 13379–13384 (2010).
7. A. Mussot, A Kudlinski, M. Droques, P. Szriftgiser, and N. Akhmediev, "Fermi-Pasta-Ulam Recurrence in Nonlinear Fiber Optics: The Role of Reversible and Irreversible Losses," Phys. Rev. X **4**, 011054 (2014).
8. T. Roger, D. Majus, G. Tamosauskas, P. Panagiotopoulos, M. Kolesik, G. Genty, A. Dubietis, and D. Faccio, "Extreme events in resonant radiation from three-dimensional light bullets," arXiv:1404.0937 [physics] (2014).
9. S. Kelly, "Characteristic sideband instability of periodically amplified average soliton," Electronics Letters **28**, 806–807 (1992).
10. N. Smith, K. Blow, and I. Andonovic, "Sideband generation through perturbations to the average soliton model," Journal of Lightwave Technology **10**, 1329–1333 (1992).
11. M. Dennis and I. Duling, I.N., "Experimental study of sideband generation in femtosecond fiber lasers," IEEE Journal of Quantum Electronics **30**, 1469–1477 (1994).
12. P. F. Curley, C. Spielmann, T. Brabec, F. Krausz, E. Wintner, and A. J. Schmidt, "Operation of a femtosecond ti:sapphire solitary laser in the vicinity of zero group-delay dispersion," Opt. Lett. **18**, 54–56 (1993).
13. S. Coen, H. G. Randle, T. Sylvestre, and M. Erkintalo, "Modeling of octave-spanning kerr frequency combs using a generalized mean-field Lugiato-Lefever model," Opt. Lett. **38**, 37–39 (2013).
14. M. R. E. Lamont, Y. Okawachi, and A. L. Gaeta, "Route to stabilized ultrabroadband microresonator-based frequency combs," Opt. Lett. **38**, 3478–3481 (2013).
15. C. Milián and D. Skryabin, "Soliton families and resonant radiation in a micro-ring resonator near zero group-velocity dispersion," Optics Express **22**, 3732 (2014).
16. M. Erkintalo, Y. Q. Xu, S. G. Murdoch, J. M. Dudley, and G. Genty, "Cascaded phase matching and nonlinear symmetry breaking in fiber frequency combs," Phys. Rev. Lett. **109**, 223904 (2012).
17. K. E. Webb, Y. Q. Xu, M. Erkintalo, and S. G. Murdoch, "Generalized dispersive wave emission in nonlinear fiber optics," Opt. Lett. **38**, 151–153 (2013).
18. M. Conforti and S. Trillo, "Dispersive wave emission from wave breaking," Opt. Lett. **38**, 3815–3818 (2013).
19. J. P. Gordon, "Dispersive perturbations of solitons of the nonlinear schrdinger equation," Journal of the Optical Society of America B **9**, 91 (1992).
20. R. Valle, "Role of the group velocity dispersion in the onset of instabilities in a nonlinear ring cavity," Optics Communications **93**, 389–399 (1992).
21. S. Malaguti, M. Conforti, and S. Trillo, "Dispersive radiation induced by shock waves in passive resonators," Opt. Lett. **39**, 5626-5629 (2014).
22. J. K. Jang, M. Erkintalo, S. G. Murdoch, and S. Coen, "Observation of dispersive wave emission by temporal cavity solitons," Opt. Lett. **39**, 5503-5506 (2014).
23. S. Wabnitz, "Suppression of interactions in a phase-locked soliton optical memory," Opt. Lett. **18**, 601–603 (1993).
24. F. Leo, S. Coen, P. Kockaert, S.-P. Gorza, P. Emplit, and M. Haelterman, "Temporal cavity solitons in one-dimensional kerr media as bits in an all-optical buffer," Nat Photon **4**, 471–476 (2010).
25. J. K. Jang, M. Erkintalo, S. G. Murdoch, and S. Coen, "Ultraweak long-range interactions of solitons observed over astronomical distances," Nat Photon **7**, 657–663 (2013).
26. N. Brauckmann, M. Kues, P. Groß, and C. Fallnich, "Adjustment of supercontinua via the optical feedback phase — experimental verifications," Opt. Express **18**, 24611–24618 (2010).
27. P. Groß, N. Haarlammert, M. Kues, T. Walbaum, and C. Fallnich, "Effects of optical feedback on femtosecond supercontinuum generation," Opt. Fiber. Technol. **18**, 290–303 (2012).
28. S. Coen, M. Haelterman, P. Emplit, L. Delage, L. M. Simohamed, and F. Reynaud, "Experimental investigation of the dynamics of a stabilized nonlinear fiber ring resonator," J. Opt. Soc. Am. B **15**, 2283–2293 (1998).
29. S. Coen and M. Haelterman, "Modulational instability induced by cavity boundary conditions in a normally dispersive optical fiber," Phys. Rev. Lett. **79**, 4139–4142 (1997).